Journal of Orthopaedics 18 (2020) 132–137

Contents lists available at ScienceDirect

Journal of Orthopaedics

journal homepage: www.elsevier.com/locate/jor

Stress shielding analysis on easy step staple prosthesis for calcaneus fractures

V. Filardi

D.A. Research and Internationalization, University of Messina, Via Consolato del mare 41, 98121, Messina, Italy

ARTICLE INFO

Keywords:
Foot model
CAD
FE analysis

ABSTRACT

Objective: The calcaneus is the most frequently injured tarsal bone, with calcaneal fractures meaning that 60% of the fractures affect the foot and about 1%–2% of all fractures.
Methods: Two 3D FE model of the foot were realized in order to compare the stress shielding occurring in a health foot and in a fractured one implanted with an easy step prosthesis by Stryker. This dispositive is indicated for calcaneus fractures.
Results: Results evidence the efficacy of this kind of prosthesis as the Eq. Von mises stresses are comparable in the two model. Higher concentration of stress are concentered on the Easy step.
Conclusion: In conclusion, the easy step staple prosthesis allows obtaining excellent results in terms of calcaneus fracture treatments. The correct implant size for a given patient can be determined by evaluating the patient's height, weight, functional demands and anatomy.

1. Introduction

The calcaneus is the most frequently injured tarsal bone, with calcaneal fractures meaning that 60% of the fractures affect the foot and about 1%–2% of all fractures. Almost 75% of calcaneal fractures have an intraarticular component. Tongue-type calcaneus fractures are longitudinal fractures that exit the calcaneal tuberosity posteriorly and involve a portion of the articular surface. They are often superiorly displaced because of the insertion of the Achilles tendon. Skin compromise complicates a large percentage of these injuries because of the thin layer of soft tissue and superficial nature of the fracture. Calcaneal fractures are the most commonly diagnosed tarsal bone fractures in emergency medicine, accounting for 60% of all tarsal fractures.[1] They frequently occur after a high-energy axial load to the heel, but can occur after relatively minor trauma.[2,3] Early recognition by the emergency physician and prompt operative repair prevent further injury and obviate the need for surgical soft tissue coverage or potential amputation. Many intra-articular fractures have important long-term consequences for patients. The treatment of displaced intra-articular calcaneal fractures is still a matter of debate. In the past, conservative treatment was advocated following the complications of surgery and the improved results with no operative treatment.

Starting from about 20 years ago, the unsatisfactory functional results after conservative treatment and routine computed tomography resulted in a reappraisal of the surgical approach. The recovery period is frequently prolonged, and a return to the pre-injury level of activity may not be reached due to pain, loss of motion, and the need for specialized footwear. However, clinical evidence supporting operative treatment for selected patient groups is limited, whereas long-term complications and adverse outcomes are still frequently documented. One of the adverse effects of the operative treatment is the damage to the soft tissues, such as flap necrosis with subsequent wound complications and sural nerve injury. To avoid these soft tissue complications, several minimally invasive procedures have been introduced. The FE analysis allows to investigate as the stress shielding can influence the design of the new prosthesis. Many FE models have been developed in order to establish the stress shielding in the bony parts or in the surgical tools.[4,5,6and7]

Greater displacement of the fracture segment and a non-fall mechanism increased the likelihood of soft tissue compromise. In those patients with threatened posterior skin, further soft tissue intervention was avoided with early reduction and immobilization. Most calcaneal fractures are splinted in the emergency setting with the ankle in a neutral position and kept immobilized by the orthopedist for several weeks to allow swelling to subside. In contrast, tongue-type calcaneus fractures should be splinted in plantar flexion to minimize soft tissue tension with emergent orthopedic consultation for open reduction and internal fixation to minimize soft tissue devitalization. In this paper a numerical comparison is proposed, evaluating the stress shielding occurring in a healthy foot subjected to 980 N, and in a fractured one. The

E-mail addresses: vfilardi@unime.it, vfilardi@unime.it.

https://doi.org/10.1016/j.jor.2019.09.008
Received 18 July 2019; Accepted 11 September 2019
Available online 12 September 2019

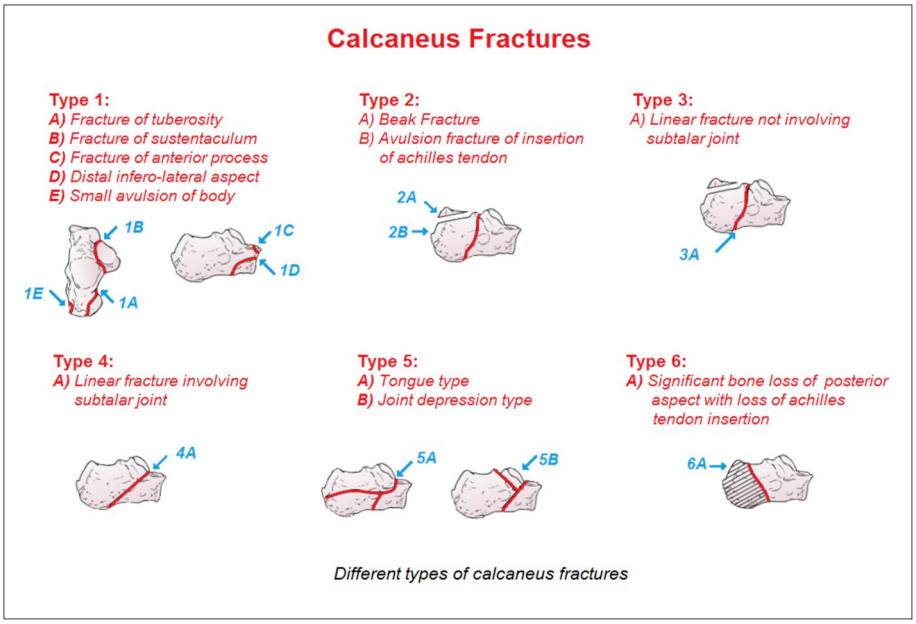

Fig. 1. Different types of calcaneus fractures.

fracture is located on the calcaneus and treated with an easy step staple prosthesis by Stryker. In Fig. 1 are depicted different types of calcaneus fractures.

2. Materials and methods

The EasyStep system is intended for bone fragment and osteotomy fixation of the foot in adult patients. Indications include: Bone fragment fixation, Osteotomy fixation. Implant selection and sizing: the correct selection of the bone fixation appliance is extremely important. Failure to use the appropriate appliance may accelerate clinical failure. Failure to use the proper component to maintain adequate blood supply and provide rigid fixation may result in loosening, bending, cracking or fracture of the device and/or bone. The correct implant size for a given patient can be determined by evaluating the patient's height, weight, functional demands and anatomy. Every implant must be used in the correct anatomic location, consistent with accepted standards of internal fixation. Two numerical models of a calcaneus fractured foot, see Fig. 2 a), and an healthy one were obtained by matching nuclear magnetic resonance (MRI) for soft tissues, and a computerized tomography (CT) for bones, carried on the two patients. In Fig. 2 b) is reported the numerical model of the fractured foot implanted with two

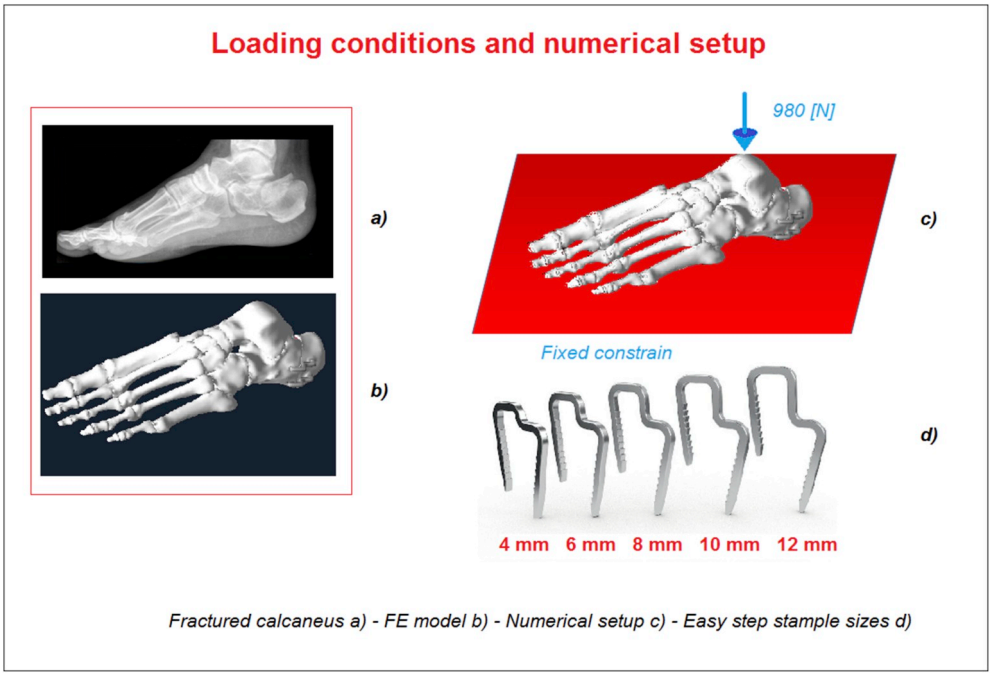

Fig. 2. Fractured calcaneus a)-FE model b)-Numerical setup c)-Easy step stample sizes d).

Table 1
FE bony segments including numbers of nodes and elements.

Bony component				
	nodes	elements	nodes	elements
Talus	4659	15192	4547	12589
Calcaneus	3423	9987	3132	9865
Navicular	1456	5212	1358	5002
Cuboid	1312	4023	1423	4125
1st Cuneiform	1232	3808	1259	3812
2nd Cuneiform	678	2096	712	2158
3rd Cuneiform	5467	16191	5377	16096
1st to 5th Metatarsal	7589	24531	7521	23564
1st to 5th Toe	6323	20896	6218	19878
Easystep staples	232	434	/	/
Rigid wall	142	612	142	612

easy step staple (size 8 mm). Models are realized with tethraedrical elements; see Table 1, ligaments, other connective tissues, and the plantar fascia were defined, by 98 truss mono dimensional elements, connecting the corresponding attachment points on the bones. All the bony and ligamentous structures were embedded in a volume of soft tissues. To simulate the frictionless contact between the joint surfaces, ABAQUS automated surface-to-surface contact option was used. According to the model developed by Gefen et al.,[8] adopting the linear elastic material law, the Young's modulus and Poisson's ratio for the bony structures were assigned as 7300 MPa and 0.3, respectively. The mechanical properties of ligaments[9] were selected from the literature, see Table 2. A load of 980 N was imposed to the talus while the complete foot was put in contact with a rigid body.[10–12]

3. Results

In Fig. 3 are reported numerical results obtained on the two FE models. As it is possible to notice the equivalent von mises stress is higher on the implanted model and its value reaches about 62 MPa. The stress registered on the healthy foot is about 33 MPa. By analyzing the picture, talus evidences a more stressed area localized on the talus and toes zone, while the implanted foot concenters its stresses on the staples. The displacements contour maps, evidenced in Fig. 4, show a more rigid behavior of the implanted foot as the maximum displacement of about 1 mm is lower than 1,2 mm resulting on the healthy foot. This trend can be explained by supposing that the specific location of the staples reduces the flexibility of the plantar arc. In Fig. 5 are reported the equivalent elastic strain contour maps. Results evidence strains localized on the implanted model reaching the 6E-003 μmm/mm while the other one reach values of about 2E-003 μmm/mm. By analyzing the picture, talus evidences a more strained area localized on the talus and toes zone, while the implanted foot concenters its stresses on the staples. Finally, in Fig. 6 are reported stresses occurring on the different parts of the implanted model. In particular, as it is possible to notice by analyzing Fig. 6 a) the Easystep staples are subjected to a stress of 62 MPa principally concentered on the curved zones. In Fig. 6 b) is depicted a stress contour maps localized on the soft tissues which reaches values of about 50 MPa.

Table 2
Mechanical and geometrical properties of the FE model.

Component	Element type	Young modulus	Poisson's ratio	Cij and Di material parameters	
Bony parts	3d Tetrahedrons	7.300 [MPa]	0.3	C_{10} = 0.08556	C_{02} = 0.00851
Soft tissue	3d Tetrahedrons	hyperelastic	/	C_{01} = -0.05841	D_1 = 3.65273
ligaments	1d Truss	350 [MPa]	/	C_{20} = 0.03900	D_2 = 0.00000
Rigid wall	3d Tetrahedrons	210.000 [MPa]	0.3	C_{11} = -0.02319	

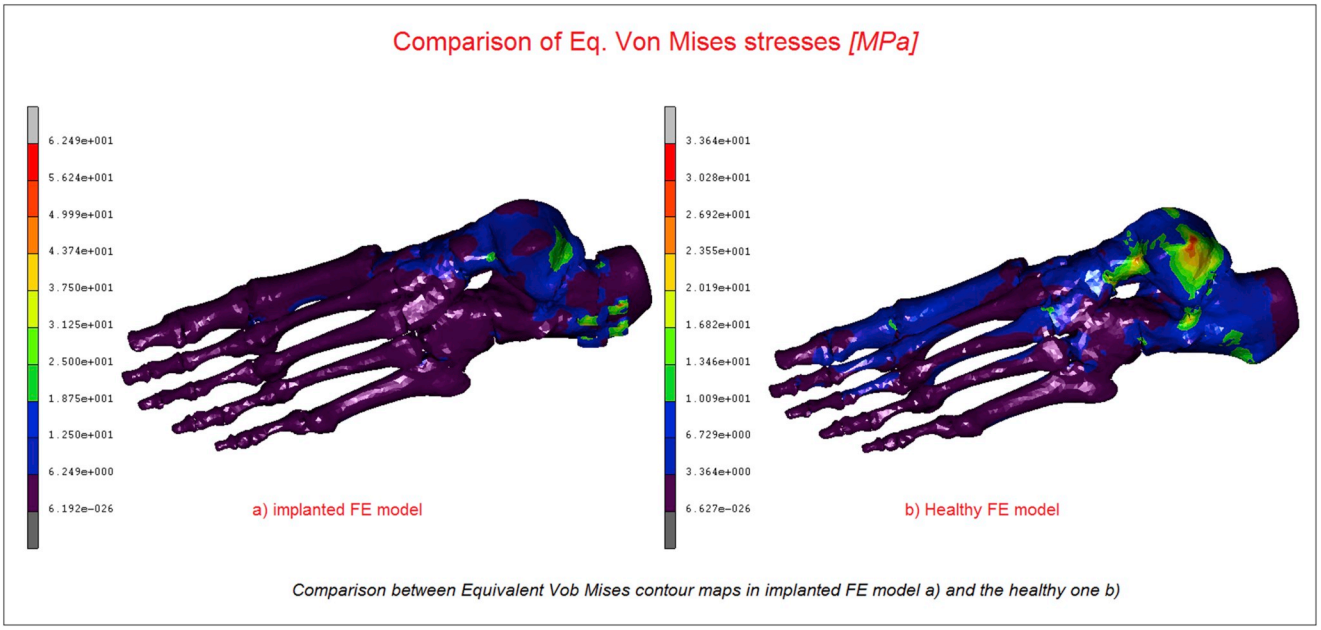

Fig. 3. Comparison between Equivalent Vob Mises contour in implanted FE model a) and the healthy one b).

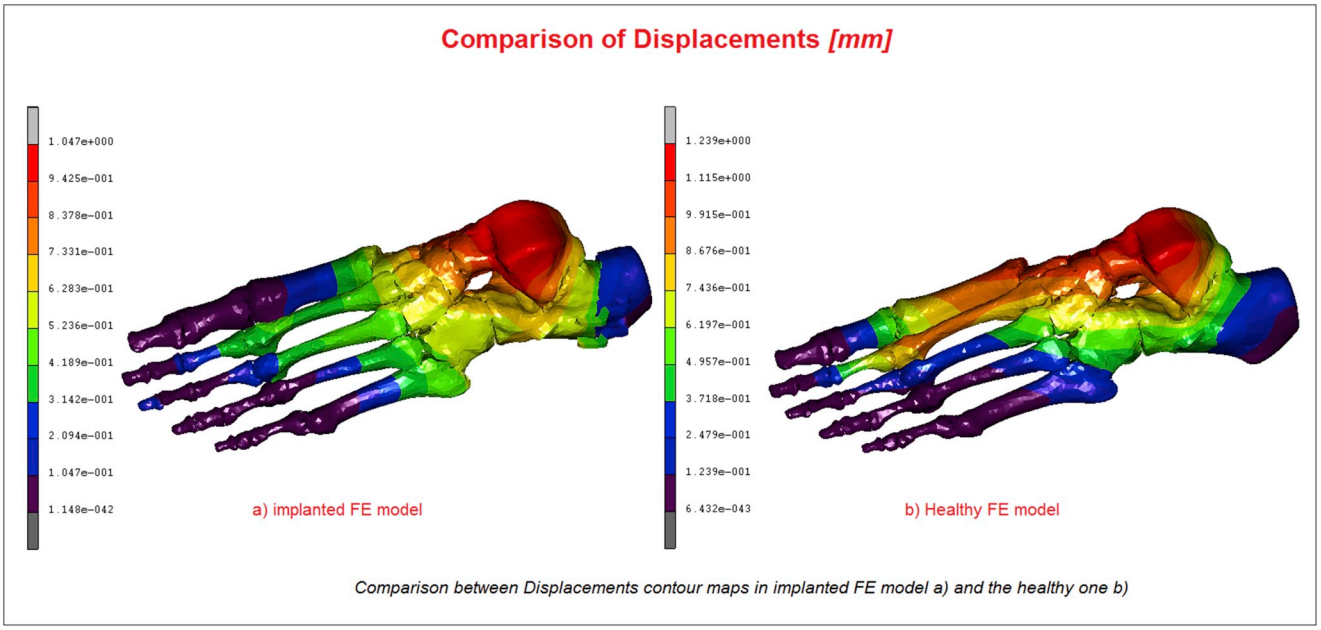

Fig. 4. Comparison between Displacement contour maps in implanted FE model a) and the healthy one b).

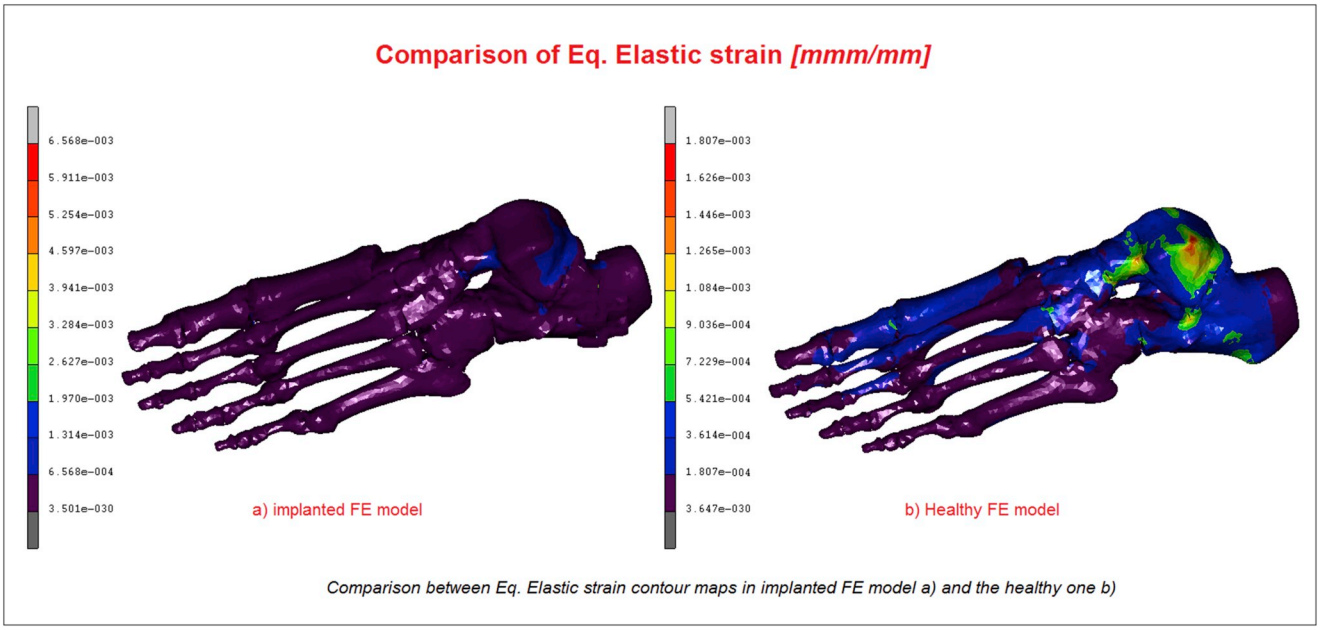

Fig. 5. Comparison between Eq Elastic strain contour maps in implanted FE model a) and healthy one b).

4. Discussion

In foot and ankle surgery, absorbable implants are used in trauma and bone operations. The modulus of elasticity of absorbable implants is close to that of cortical bone, which makes them safe for internal ankle or calcaneal fractures. Because absorbable implants are weaker than metallic ones, patients with calcaneal fractures fixed by absorbable implants have their rehabilitation restricted early on to avoid implant breakage and bone refractures.[13] Wang et al.[14] compared the strength of two types of fixation method for calcaneal fractures. Redfen et al.[15] compared the mechanical integrity of locking plate and traditional non-locking plate fixation for calcaneal fractures. Nelson et al.[16] evaluated the stability of a new headless screw technique for calcaneal fractures. Richter et al.[17] compared the stability of a calcaneal plate with polyaxially locked screws with 3 plates fixed with uniaxially locked screws. All these studies used cadaveric or physical models to reconstruct the fractures and fixation. However, few parameters can be measured through mechanical experiments and experimental cost is very high. Many important parameters, such as displacement, stress, and strain at any location, are difficult to measure using current techniques. In FE calculation, the stress at the connections of different materials has a larger computational error than that for homogeneous materials. Although the computational error often results in higher stress, comparisons of stress between screws in a given model can produce useful results. Plantar fasciitis is mainly associated with athletes, but it can affect anyone involved in intensive physical activities. A significant decrease of the arch height post-surgery, as predicted by the model, may reduce the dynamic shock-absorbing abilities of the foot,

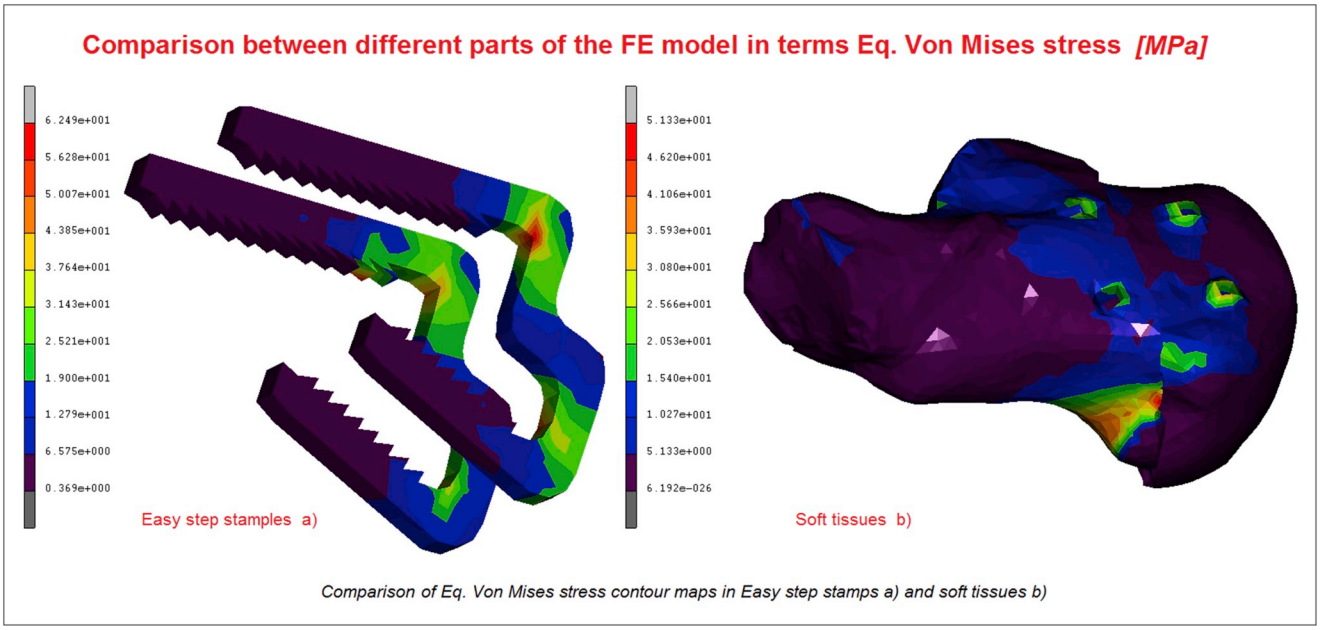

Fig. 6. Comparison of Eq Von Mises stress contours mapls in Easy step stamps a) and soft tissues b).

and cause further musculoskeletal damage, as shown in clinical studies where subjects with flat feet could not sustain long marches, and were at higher risks for developing stress fractures.[18] Moreover, the plantar fascia has an important role in relieving metatarsal stresses. The dorsal aspects of the medial metatarsals are normally loaded in compression (Fig. 3). Removal of the fascia elevated the bending loads on these bones, and, thereby, increased the dorsal compression stresses by as much as 65%. This suggests that release of the fascia will accelerate fatigue damage to these bones during intensive activity such as marching and hence, when surgical removal or significant release of the fascia is considered, a decrease in the foot's abilities of load-bearing and shock-attenuation should be taken into account. Tongue type calcaneal fractures, in contrast to the more common joint depression patterns, are longitudinal fractures that involve the calcaneal tuberosity and a portion of the posterior articular facet. Superior and dorsal displacement of the calcaneal tuberosity fragment is common because of rotation of the fracture fragment from the pull of the soleus complex. This displacement can potentially tent the relatively thin skin of the posterior heel and place it under significant tension, eventually leading to partial- or full-thickness necrosis.[19,20] Other FE models were proposed for studying the entire bony chain of leg taking into account[21–24] stress occurring in healthy feet, examining various applications. Other researches[25–27] presented an FE foot model based on MR images investigating the stress map distribution on the different bony part of the foot.

5. Conclusion

Analytical models allow to determinate physical conditions of solid or fluid components, for example analysis can investigate artery deseases.[28,29] The model presented in this work may be further applied to investigate numerous acquired foot deformities or traumatic injuries, and the mechanisms acting in such conditions could be studied by altering its geometrical or material properties. Moreover, various new or conservative surgical interventions could be evaluated by removing or adding elements to the computational simulation. Orthotics and supportive devices may also be assessed, and their effect on the internal and foot-ground contact stress distributions can be studied. When used together with FGP experimental measurements, the present computational foot model can be a highly effective biomechanical tool with clinical applications in pre- and post-treatment evaluations.

References

1. Simon RR, Sherman SC. *Emergency Orthopedics.* sixth ed. New York: McGraw-Hill; 2011.
2. Gardner MJ, Nork SE, Barei DP, Kramer PA, Sangeorzan BJ, Benirschke SK. Secondary soft tissue compromise in tongue-type calcaneus fractures. *J Orthop Trauma.* 2008;22(7):439–445.
3. Hess M, Booth B, Laughlin R. Calcaneal avulsion fractures: complications from delayed treatment. *Am J Emerg Med.* 2008;26:54 e1–4.
4. Filardi V. The healing stages of an intramedullary implanted tibia: a stress strain comparative analysis of the calcification process. *J Orthop.* 2015;12:51–61.
5. Filardi V. Characterization of an innovative intramedullary nail for diaphyseal fractures of long bones. *Med Eng Phys.* 2017;49(1):94–102.
6. Filardi V. Healing of femoral fractures by the meaning of an innovative intramedullary nail. *J Orthop.* 2018;15(1):73–77.
7. Filardi V. Numerical comparison of two different tibial nails: expert tibial nail and innovative nail. *Int J Interact Des Manuf.* 2018;12(4):1435–1445.
8. Gefen A, Megido-Ravid M, Itzchak Y, Arcan M. Biomechanical analysis of the threedimensional foot structure duringg ait: a basic tool for clinical applications. *J Biomech Eng.* 2000;122:630–639.
9. Siegler S, Block J, Schneck CD. The mechanical characteristics of the collateral ligaments of the human ankle joint. *Foot Ankle.* 1988;8:234–242.
10. Filardi V. Healing of tibial comminuted fractures by the meaning of an innovative intramedullary nail. *J Orthop.* 2019;16(2):145–150.
11. Filardi V, Montanini R. Measurement of local strains induced into the femur by trochanteric Gamma nail implants with one or two distal screws. *Med Eng Phys.* 2007;29(1):38–47.
12. Montanini R, Filardi V. In vitro biomechanical evaluation of antegrade femoral nailing at early and late postoperative stages. *Med Eng Phys.* 2010;32(8):889–897.
13. Zhang J, Xiao B, Wu Z. Surgical treatment of calcaneal fractures with bioabsorbable screws. *Int Orthop.* 2011;35:529–533.
14. Wang CL, Chang GL, Tseng WC, Yu CY, Lin RM. Strength of internal fixation for calcaneal fractures. *Clin Biomech.* 1998;13:230–233.
15. Redfern DJ, Oliverira ML, Campbell JT, Belkoff SM. A biomechanical comparison of locking and non- locking plates for the fixation of calcaneal fracture. *Foot Ankle Int.* 2006;27:196–201.
16. Nelson JD, Mclff TE, Moodie PG, Iverson JL, Horton GA. Biomechanical stability of intramedullary technique for fixation of joint depressed calcaneus fracture. *Foot Ankle Int.* 2010;31:229–235.
17. Richter M, Droste P, Goesling T, Zech S, Krettek C. Polyaxially-locked plate screws increase stability of fracture fixation in an experimental model of calcaneal fracture. *J Bone Jt Surg.* 2006;88:1257–1263.
18. Brosh T, Arcan M. Toward early detection of the tendency to stress fractures. *Clin Biomech.* 1994;9:111–116.
19. Squires B, Allen PE, Atkins RM. Fractures of the tuberosity of the calcaneus. *J Bone Jt. Surg.* 2001;83(1):55–61.
20. Watson TS. Soft tissue complications following calcaneal fractures. *Foot Ankle Clin.* 2007;12:107–123.
21. Filardi V. FE analysis of stress and displacements occurring in the bony chain of leg. *J Orthop.* 2014;11(4):157–165.

22. Filardi V, Simona P, Cacciola G, ... Milardi D, Alessia B. Finite element analysis of sagittal balance in different morphotype: forces and resulting strain in pelvis and spine. *J Orthop*. 2017;14(2):268–275.
23. Filardi V, Milardi D. Experimental strain analysis on the entire bony leg compared with FE analysis. *J Orthop*. 2017;14(1):115–122.
24. Filardi V. Stress shielding in the bony chain of leg in presence of varus or valgus knee. *J Orthop*. 2015;12(2):102–110.
25. Filardi V. Flatfoot and normal foot a comparative analysis of the stress shielding. *J Orthop*. 2018;15(3):820–825.
26. Filardi V. Finite element analysis of the foot: stress and displacement shielding. *J Orthop*. 2018;15(4):974–979.
27. Filardi V. Tibio talar contact stress: An experimental and numerical study. *J Orthop*. 2019. https://doi.org/10.1016/j.jor.2019.08.024.
28. Filardi V. Carotid artery stenosis near a bifurcation investigated by fluid dynamic analyses. *Neuroradiol J*. 2013;26(4):439–453.
29. Filardi V. CFD analysis to evaluate hemodynamic parameters in a growing abdominal aortic aneurysm. *Vasc Dis Manag*. 2015;12(5):84–95.